Exchange of Gating Properties Between Rat Cx46 and Chicken Cx45.6

Jun-Jie Tong, Xiaoqin Liu, Lixian Dong, and Lisa Ebihara
Department of Physiology and Biophysics, Rosalind Franklin School of Medicine and Science, North Chicago, Illinois

ABSTRACT Cx46 and Cx50 are coexpressed in lens fiber cells where they form fiber-fiber gap junctions. Recent studies have shown that both proteins play a critical role in maintaining lens transparency. Although both Cx46 and Cx50 (or its chicken ortholog, Cx45.6) show a high degree of sequence homology, they exhibit marked differences in gap junctional channel gating, unitary gap junctional channel conductance, and hemichannel gating. To better understand which regions of the protein are responsible for these functional differences, we have constructed a series of chimeric Cx46-Cx45.6 gap junctional proteins in which a single transmembrane or intracellular domain of Cx45.6 was replaced with the corresponding domain of Cx46, expressed them in *Xenopus* oocyte pairs or N2A cells, and examined the resulting gap junctional conductances. Our results showed that four out of six of the chimeras induced high levels of gap junctional coupling. Of these chimeras, only Cx45.6-46NT showed significant changes in voltage-dependent gating properties. Exchanging the N-terminus had multiple effects. It slowed the inactivation kinetics of the macroscopic junctional currents so that they resembled those of Cx46, reduced the voltage sensitivity of the steady-state junctional conductance, and decreased the conductance of single gap junctional channels. Additional point mutations identified a uniquely occurring arginine in the N-terminus of Cx46 as the main determinant for the change in voltage-dependent gating.

INTRODUCTION

Gap junctions are membrane specializations containing intercellular channels that allow the passage of ions and other low-molecular weight molecules between adjacent cells. These channels are composed of proteins called connexins that are members of a multigene family with at least 20 human members (Willecke et al., 2002).

Three different connexins have been identified in the mammalian lens: Cx43, Cx46, and Cx50 (Beyer et al., 1987; Paul et al., 1991; White et al., 1992). Cx43 is expressed primarily in the epithelial cells, whereas Cx46 and Cx50 are coexpressed in fiber cells. All three of these gap junctional proteins are believed to play an important role in maintaining metabolic homeostasis in the lens. It has recently been shown that mutations in the genes for Cx50 and Cx46 are associated with congenital cataracts in humans (Shiels et al., 1998; Mackay et al., 1999). Furthermore, studies on genetically manipulated mice demonstrate that disruption of the gene for either Cx50 or Cx46 by homozygous knockout leads to the development of cataracts in mice (Gong et al., 1997; White et al., 1998). However, the mice had different phenotypes. Cx50 knockout mice exhibited mild nuclear cataracts and microopthalmia. In contrast, Cx46 knockout mice developed severe nuclear cataracts but lens and eye growth were normal. Replacement of Cx50 with Cx46 by knockin rescued lens clarity but could not restore normal growth, suggesting that the two connexins may be tailored to serve specific functions in the lens (White, 2002).

The functional properties of gap junctional channels formed by Cx50 and Cx46 have been examined in communication-deficient mammalian cell lines and *Xenopus* oocyte pairs using electrophysiological techniques (White et al., 1994; Paul et al., 1991; Srinivas et al., 1999; Hopperstad et al., 2000; Xu and Ebihara, 1999; Eckert, 2002; Sakai et al., 2003). These studies show that although Cx50 and Cx46 have very similar amino acid sequences, their gap junctional channels exhibit marked differences in voltage-gating properties and single-channel conductance. Furthermore, single oocytes injected with cRNA for Cx50 or Cx46 develop calcium-sensitive hemichannel currents with distinct voltage-gating properties (Ebihara and Steiner, 1993; Beahm and Hall, 2002).

The N-terminus may play an important role in voltage-dependent gating of gap junctional channels. Previous mutational studies of Cx32 and Cx26 have shown that charged amino acids in the N-terminus determine the polarity of V_j-gating (Verselis et al., 1994; Oh et al., 2000; Purnick et al., 2001). More recently, Musa et al. (2004) reported that two charged amino acids in the N-terminus of Cx40 and Cx43 control the V_j-gating polarity and block by spermine of these connexins. In this study, we constructed a series of chimeras composed of segments of rat Cx46 and chicken Cx45.6, which is a species ortholog of mouse Cx50 (Jiang et al., 1994), expressed them in *Xenopus* oocyte pairs or N2A cells, and examined the resulting gap junctional conductances. Our results demonstrate that the N-terminus is largely responsible for the change in voltage-gating properties. In addition, exchanging the N-terminus modifies single gap junctional channel conductance.

Submitted January 7, 2004, and accepted for publication July 7, 2004.

Address reprint requests to Lisa Ebihara, Finch University of Health Sciences, The Chicago Medical School, Dept. of Physiology and Biophysics, 333 Green Bay Rd., North Chicago, IL 60064. Tel.: 847-578-3424; E-mail: lisa.ebihara@rosalindfranklin.edu.

0006-3495/04/10/2397/10 $2.00

doi: 10.1529/biophysj.104.039594

METHODS

Construction of chimeric and mutant subunits

We constructed six chimeric constructs in which a single domain of chicken Cx45.6 was replaced by the corresponding domain of rat Cx46 using PCR amplification. The domains of the two connexins, based on the alignment published by Bennett et al. (1991) are delimited as follows. Cx46 is divided into N (Met1–Lys23), M1 (Val24–Ala41), E1 (Glu42–Arg76), M2 (Phe77–Gly94), L (His95–Ala150), M3 (Leu151–Phe169), E2 (Ile170–Thr207), M4 (Ile208–Leu226), and CT (Glu227–Ile416). Cx45.6 is divided into N (Met1–Arg23), M1 (Val24–Ala41), E1 (Glu42–Arg76), M2 (Leu77–Gly94), L (His95–Thr148), M3 (Leu149–Phe167), E2 (Ile168–Thr205), M4 (Ile206–Val224), and CT (Glu225–Val400).

To generate the Cx45.6-46NT construct, two primers were synthesized to amplify the DNA encoding the N-terminus (NT) of Cx46: sense 5′-CAATTAGGCTTGTACATATTGTCGTTAGAACGC-3′; and antisense, 5′-CAGCACCAGAATTCGAAAGATGAACAGGAC-GGTC-3′. The sense primer corresponded to a region of the transcription vector, SP64T, containing a naturally occurring BsrGI restriction site. The antisense primer corresponded to codons 27–37 in M1 of Cx46. The nucleotide sequence of codons 32–34 in the antisense primer were modified to create a BstBI restriction site without changing the predicted amino acid sequence (PheArgIle). A second set of primers was designed to amplify Cx45.6 sequences, as well as the transcription vector, SP64T, in which Cx45.6 was subcloned: sense, 5′-CTCTTCATTTTTCGAATCCT-GATCCTGGGAACGGCTG-3′; and antisense, 5′CGACAATATGTACA-AGCCTAATTGTGTAGCATCTG-3′. The sense primer corresponded to the last 12 codons in M1 of Cx45.6. The codons for the conserved PheArgIle sequence in Cx45.6's M1 were also modified to generate a BstBI restriction site without changing the predicted amino acid sequence. DNA amplification was performed with PfuTurbo DNA Polymerase (Stratagene, La Jolla, CA) according to the manufacturer's protocol in a thermocycler (PTC-150, MJ Research, Watertown, MA). The PCR products were digested with BsrGI and BstBI, gel purified, and ligated together to generate a chimera in which the N-terminus of Cx45.6 (amino acids 1–23) was replaced with the corresponding NT of Cx46. A similar strategy was used to generate the other chimeras. Point mutations were generated using the QuikChange Site-Directed Mutagenesis Kit (Stratagene) according to the manufacturer's protocol. All of the constructs were sequenced (DNA Sequencing and Synthesis Facility, Iowa State University, Ames, IA) to ensure that PCR amplification did not introduce random mutations.

Expression of connexins in *Xenopus* oocytes

Adult female *Xenopus laevis* frogs were anesthetized on ice and a partial ovarectomy performed. The oocytes were defolliculated by treating them with collagenase IA (Sigma Chemical, St. Louis, MO). Stage V and VI oocytes were selected and pressure injected using a Nanoject variable microinjection apparatus (model 3-000-203, Drummond Scientific, Broomal, PA) with 0.23 ng of oligonucleotides antisense to mRNA for *Xenopus* Cx38 as previously described (Ebihara, 1996). The oocytes were incubated overnight at 18°C in Modified Barth's Solution containing (in mM) 88 NaCl, 1 KCl, 2.4 $NaHCO_3$, 15 Hepes, .3 $CaNO_3 \times 4H_2O$, 0.41 $CaCl_2 \times 6H_2O$, 0.82 $MgSO_4 \times H_2O$, 550 mg/L pyruvate and 50 μg/ml gentamycin, pH 7.4. Connexin cRNAs were synthesized using the mMessage mMachine in vitro transcription kit (Ambion, Austin, TX) according to the manufacturer's instructions. The amount of cRNA was quantitated by measuring the absorbance at 260 nm. The purity and amount of cRNA was further assessed by agarose gel electrophoresis. Cx38 antisense-pretreated oocytes were injected with 36 nl of 0.04–4 ng/nl connexin cRNA and incubated for an additional 16–24 h at 18°C in Modified Barth's Solution containing 5 mM $CaCl_2$.

Expression of connexins in N2A cells

N2A mouse neuroblastoma cells were grown in Dulbecco's minimal essential medium (Life Technologies, Gaithersburg, MD) containing 10% fetal bovine serum, 2 mM L-Glutamine, 100 units/ml penicillin G and 100 μg/ml streptomycin sulfate in a humidified 5% CO_2 incubator at 37°C.

For transient transfections, N2A cells (grown to ~60% confluence on lysozyme-treated coverslips in 35-mm tissue dishes) were cotransfected with 1 μg of Cx45.6 or Cx45.6-46NT cDNA and 1 μg of enhanced green fluorescence protein (EGFP) cDNA using Superfect reagent (Qiagen, Valencia, CA) following the manufacturer's protocol. Electrophysiological recordings were performed 18–72 h later. Cell pairs expressing exogenous connexins were identified by EGFP fluorescence using a Nikon Diaphot microscope (equipped with a mercury arc lamp and fluorescein isothiocyanate filter sets).

Electrophysiological measurement and analysis of gap junctional currents expressed in *Xenopus* oocytes

For gap junctional conductance measurement, connexin cRNA-injected oocytes were manually devitellinized and paired as previously described (Ebihara, 1992). The oocyte pairs were allowed to incubate at room temperature for 2–4 h (or in some cases overnight) before electrophysiological recording. Double two-microelectrode voltage-clamp experiments were performed using a Gene-Clamp 500 and an Axoclamp 2A voltage-clamp amplifier (Axon Instruments, Union City, CA). The microelectrodes were filled with 3 M KCl and had resistances between 0.1 and 0.6 MΩ. To prevent electrode leakage, the tips of the electrodes were backfilled with 1% agar in 3 M KCl. For simple measurements of gap junctional coupling, both cells of the pair were initially held at −40 mV and 5- to 10-mV steps were applied to one cell while holding the second cell at −40 mV. Under these conditions, the change in current measured in the second cell would be equal to the junctional current (I_j). The junctional conductance (G_j) was calculated as ($G_j = I_j/V_j$), where $V_j = V_{cell\ 2} - V_{cell\ 1}$. To determine the voltage-dependent gating properties of the gap junctions, families of junctional current traces were recorded in oocyte pairs by applying transjunctional voltage-clamp steps between +90 mV and −90 mV in decrements of 20 mV. Changes in junctional conductance during the experiment were monitored by applying a 5-mV prepulse of 1-s duration 1 s before the initiation of the test pulse. Only cell pairs with junctional conductances <7 μS were selected for analysis. The instantaneous junctional current ($I_{j,inst}$) was determined by fitting the junctional current traces to the sum of two exponentials and extrapolating back to the beginning of the voltage-clamp pulse. The steady-state junctional current ($I_{j,ss}$) was determined at the end of the pulse. Instantaneous conductance ($G_{j,inst}$) was calculated for each voltage trace as ($G_{j,inst} = I_{j,inst}/V_j$) and normalized to the conductance of the prepulse for each trace. The normalized steady-state junctional conductance ($G_{j,ss}$) was calculated as ($G_{j,ss} = I_{j,ss}/I_{j,inst}$). The relationship between $G_{j,ss}$ and V_j was fit using a two-state Boltzmann equation (Spray et al., 1981):

$$G_{j,ss} = \{(G_{max} - G_{min})/(1 + \exp(A(V_j - V_0)))\} + G_{min},$$

where V_0 is the voltage at which the steady-state junctional conductance is half of its maximum value, A is a parameter that defines the steepness of voltage sensitivity, G_{max} is the maximum normalized conductance, and G_{min} is the minimum normalized conductance. A can also be expressed as a gating charge, z, where $z = A(kT)/q$, k is the Boltzmann constant, T = absolute temperature, and q = elementary charge.

Pulse generation and data acquisition were performed using a PC computer equipped with PCLAMP 6 software and a TL-1 acquisition system (Axon Instruments). Currents were filtered at 20–50 Hz and digitized using PCLAMP6 software and a Digidata 1200 interface (Axon Instruments). All experiments were performed at room temperature (20–22°C).

Electrophysiological measurement and analysis of gap junctional channels expressed in N2A cells

Junctional currents were recorded from transiently transfected N2A cell pairs using the dual whole-cell patch-clamp technique (Neyton and Trautmann, 1985) and two patch-clamp amplifiers (Axopatch 200A, Axon Instruments; and EPC-7, List Electronic, Darmstadt, Germany). Patch pipettes were pulled from glass capillaries on a Flaming/Brown Micropipette puller (model P-87; Sutter Instruments, Novato, CA). The patch electrodes had resistances of 3–8 MΩ when filled with standard internal solution containing (in mM) 130 CsCl, 10 EGTA, 0.5 $CaCl_2$, 3 MgATP, 2 Na_2ATP, 10 HEPES, pH 7.5. The extracellular solution contained (in mM) 140 NaCl, 2 CsCl, 2 $CaCl_2$, 1 $MgCl_2$, 4 KCl, 5 dextrose, 2 pyruvate, 1 $BaCl_2$, 5 HEPES, pH 7.5, To measure gap junctional conductance, both cells of a pair were initially held at a common holding potential of 0 mV. Voltage pulses of 4- to 8-s duration between 100 mV and −100 mV were applied to one cell whereas the second cell was held at 0 mV. Gap junctional current was recorded in the second cell of the pair. The normalized steady-state junctional conductance ($G_{j,ss}$) was determined by dividing the steady-state current (measured at 8 s) by the initial current. No series compensation was used. Only cell pairs having conductances <7 nS were selected for data analysis to minimize series resistance artifacts.

Single-channel data were obtained from cell pairs that had only one or two functional channels using voltage-clamp protocols as described above. All-amplitude histograms were constructed from the patch-clamp records and fit to the sum of Gaussians to determine the amplitude of the current during channel openings. Data was acquired using a PC computer equipped with a Digidata 1320A interface and PCLAMP8 or 9 software (Axon Instruments). The current signal was filtered at 1 kHz and digitized at 5 kHz.

RESULTS

Expression of wild-type and chimeric lens connexins in *Xenopus* oocytes

Our initial experiments confirmed that there was a marked difference in macroscopic kinetics between homotypic gap junctional channels formed from wild-type rat Cx46 and chicken Cx45.6 (Fig. 1, *A* and *B*, Table 1). Cx45.6 junctional currents inactivated rapidly at larger transjunctional potentials ($|V_j| > 30$ mV). The time course of decay could be described by the sum of two exponentials with $\tau_1 = 80.7 \pm 10.3$ ms and $\tau_2 = 1926.7 \pm 123.9$ ms at $V_j = -90$ mV. In contrast, Cx46 junctional currents inactivated slowly ($\tau_1 = 437.7 \pm 58.6$ ms and $\tau_2 = 2023.6 \pm 46.7$ ms at $V_j = -90$ mV). The two types of channels also showed differences in steady-state conductance-voltage relationships, which were quantified by fitting the data to a Boltzmann equation (Table 2). The conductance-voltage relationship of Cx45.6 showed a more pronounced voltage sensitivity (half-inactivation potential, $V_0 = 35.4$ mV, slope factor, $A = .149$) than Cx46 junctions ($V_0 = 59.5$ mV, A = .084).

To determine the structural basis of the different gating kinetics of Cx46 and Cx45.6 channels, we constructed a series of six chimeric Cx46-Cx45.6 gap junctional proteins in which a single transmembrane or intracellular domain of Cx45.6 was replaced with the corresponding domain of Cx46. The chimeric connexins were subsequently expressed in *Xenopus* oocytes and tested for gap junctional coupling 16–24 h after pairing. Our results show that four out of six of the chimeras induced high levels of gap junctional coupling with junctional conductances ranging between 8 and 32 μS (Table 3). Of these chimeras, only Cx45.6-46NT showed significant changes in voltage-dependent gating properties (see Tables 1 and 2). Fig. 1 *C* shows a family of macroscopic gap junctional current traces recorded from a homotypic Cx45.6-46NT cell pair. Exchanging the N-terminus slowed the inactivation kinetics of the junctional currents so that they resembled those of Cx46. This can be better seen in Fig. 2, which compares the time course of inactivation of wild-type and Cx45.6-46NT junctional currents at a transjunctional potential of −90 mV. The time course of current relaxation at −70 and −90 mV was quantified by fitting the data to

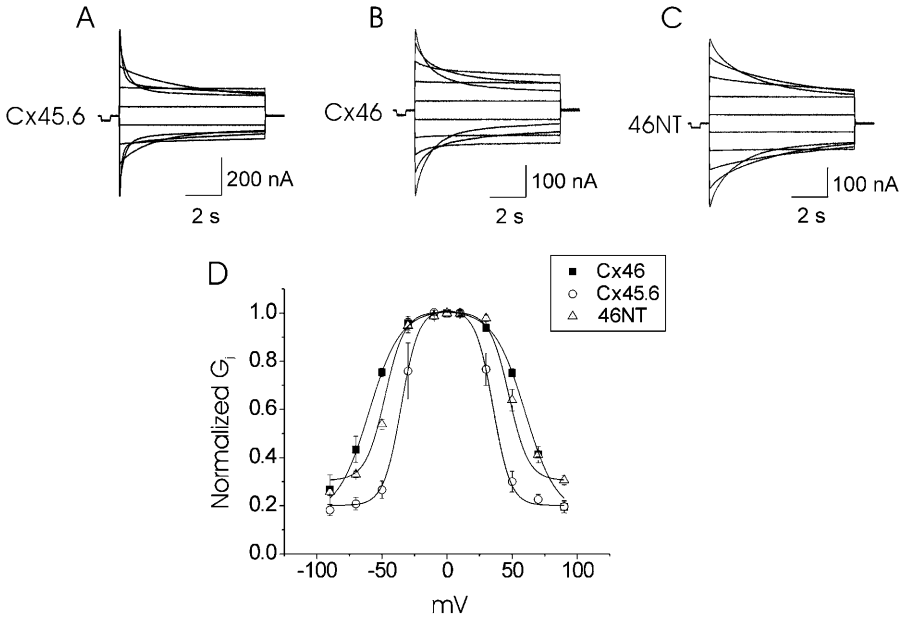

FIGURE 1 Gap junctions formed from Cx45.6-46NT exhibit voltage-dependent gating properties that resemble those of Cx46. (*A–C*) Representative families of junctional current traces recorded from oocyte pairs expressing Cx45.6 (*A*), Cx46 (*B*), or Cx45.6-46NT (*C*) in response to transjunctional voltage-clamp steps from 90 mV to −90 mV in 20-mV decrements. (*D*) Plots of normalized steady-state junctional conductance versus transjunctional voltage for Cx46 (*solid squares*), Cx45.6 (*open circles*), and 46NT (*open triangles*). Points represent the mean ± SE. The solid lines are the best fit of the data to Boltzmann equations whose parameters are given in Table 2.

TABLE 1 Time constants of inactivation

Homotypic oocyte pairs

	−90 mV, 4 s			−70 mV, 4 s		
Cx	A_{fast}/A_{slow}	τ_{fast} (ms)	τ_{slow} (ms)	A_{fast}/A_{slow}	τ_{fast} (ms)	τ_{slow} (ms)
Cx45.6	5.22 ± 0.3	80.7 ± 10.3	1926.7 ± 123.9	5.84 ± 2.06	177.1 ± 40.2	1612.6 ± 396.8
46loop	1.95 ± 0.05	78.6 ± 1.16	1457.6 ± 19.9	3.11 ± 0.28	113.4 ± 15.9	1142.4 ± 33.0
46M3	5.25 ± 0.87	72.1 ± 6.06	1821.4 ± 49.3	6.84 ± 1.54	143.0 ± 35.2	1590.3 ± 242.6
46M4	3.92 ± 1.75	68.6 ± 3.41	1733.9 ± 187.7	4.6 ± 0.46	126.7 ± 13.8	924.3 ± 118.7
	−90 mV, 8 s			−70 mV, 8 s		
Cx	A_{fast}/A_{slow}	τ_{fast} (ms)	τ_{slow} (ms)	A_{fast}/A_{slow}	τ_{fast} (ms)	τ_{slow} (ms)
Cx46	1.03 ± .16	437.7 ± 58.6	2023.6 ± 46.7	0.62 ± .125	465.7 ± .5	2721.0 ± 339.2
46NT	.695 ± .26	375.7 ± 9.0	1805.4 ± 73.6	.245 ± .064	381.3 ± 34.2	3314.4 ± 321.1
N9R	1.98 ± 0.75	419.1 ± 31.7	1903.1 ± 125.4	0.17 ± 0.04	317.7 ± 39.8	3111.6 ± 489.1

Heterotypic oocyte pairs

	−90 mV, 8 s			−70 mV, 8 s		
Cx	A_{fast}/A_{slow}	τ_{fast} (ms)	τ_{slow} (ms)	A_{fast}/A_{slow}	τ_{fast} (ms)	τ_{slow} (ms)
Cx45.6/46NT(−)*	3.5 ± 0.16	89.7 ± 4.4	1022.1 ± 45.4	2.6 ± 0.28	155.0 ± 3.3	1027.3 ± 23.8
Cx45.6/46NT(+)*	1.0 ± 0.14	229.8 ± 7.5	946.4 ± 21.9	0.37 ± 0.05	239.8 ± 20.6	1458.2 ± 47.3

For kinetic analysis, the junctional current from three or four pairs of each group was fit to the equation $I_j = A_{fast}e^{(-t/\tau_{fast})} + A_{slow}e^{(-t/\tau_{slow})}$. All values are given as mean ± SE.

*Voltage polarity is relative to the cell expressing 46NT.

a biexponential function. The time constants of inactivation for Cx45.6-46NT were not statistically different from those for Cx46 (Table 1). The steady-state G_j-V_j relationship was also modified. The junctional conductance showed a voltage sensitivity that was intermediate between that of Cx45.6 and Cx46 (Table 2).

To better understand how the N-terminus influences gap junctional channel gating, we examined the properties of heterotypic gap junctions formed by Cx45.6 and Cx45.6-46NT. Fig. 3 *A* shows gap junctional current traces recorded from heterotypic pairs. In these experiments, the voltage-clamp pulses were applied to the cell expressing Cx45.6-

TABLE 2 Boltzmann parameters of connexins expressed in *Xenopus* oocytes and transiently transfected N2A cells

Homotypic oocyte pair

Cx	A	z	V_o(mV)	G_{min}	G_j (μS) mean ± SE	Number of pairs analysed
Cx46	.083	2.1	60.0	.166	3.04 ± .39	3
Cx45.6	.149	3.8	35.41	.201	4.41 ± .64	4
46NT	.134	3.4	47.6	.306	2.4 ± .43	3
N9R	.090	2.3	48.61	.300	2.7 ± .34	6
46loop	.161	4.1	29.05	.218	4.81 ± .45	4
46M3	.141	3.6	31.0	.179	5.05 ± .77	5
46M4	.117	3.0	35.84	.226	4.12 ± .98	4

Heterotypic oocyte pairs

Cx	A	z	V_o (mV)	G_{min}	G_j (μS) mean ± SE	Number of pairs analysed
Cx45.6/46NT(−)*	.157	4.0	−37.0	.20	3.1±.52	5
Cx45.6/46NT(+)*	.114	2.9	45.2	.29		

Homotypic N2A cell pairs

Cx	A	z	V_o (mV)	G_{min}	G_j (nS) mean ± SE	Number of pairs analyzed
Cx45.6	.175	4.4	39.3	.22	3.82 ± 0.16	3
Cx46†	.08	2.0	48.1	.11		
46NT	.078	2.0	58.6	.23	1.26 ± 0.29	6

*Voltage polarity is relative to the cell expressing 46NT.

†Cx46 data are from Hopperstad et al. (2000).

TABLE 3 Gap junctional coupling of paired *X. laevis* oocytes expressing wild-type and chimeric connexins

Oocyte injection cell 1/cell 2	G_j (μS) mean ± SE	No. of pairs tested
wtCx46/wtCx46	9.67 ± 2.105	8
wtCx45.6/wtCx45.6	9.28 ± 2.37	4
Cx45.6-46NT/Cx45.6-46NT	20.4 ± 8.47	12
Cx45.6-46M1/Cx45.6-46M1	Not tested*	
Cx45.6-46M2/Cx45.6-46M2	.043 ±.01	5
Cx45.6-46loop/Cx45.6-46loop	8.057 ± 4.73	6
Cx45.6-46M3/Cx45.6-46M3	18.55 ± 2.54	7
Cx45.6-46M4/Cx45.6-46M4	32.14 ± 7.245	13
AS/AS	.069 ± .009	16

Oocytes were paired and incubated at 18°C for 24 h before measurement of gap junctional coupling.
*Oocytes injected with cRNA for Cx45.6-46M1 developed a large, voltage-independent membrane conductance that could not be blocked by incubation in elevated $[Ca^{2+}]_o$.

46NT while holding the cell expressing Cx45.6 at a constant membrane potential. Heterotypic junctions closed more rapidly when negative voltage-clamp pulses were applied to the Cx45.6-46NT-containing cell. The voltage dependence of the fast time constant of inactivation resembled that of Cx45.6-46NT and Cx45.6 at positive and negative potentials, respectively (Fig. 3 *C*). The steady-state G_j-V_j relationship was also asymmetrical (Fig. 3 *B*). The negative limb of the G_j-V_j relationship was steeper and had a smaller $G_{j,min}$ (Table 2). Comparison of the Boltzmann parameters of the heterotypic junctions with those of the homotypic junctions showed that the positive limb of the G_j-V_j relationship resembled that of Cx45.6-46NT, whereas the negative limb resembled that of Cx45.6.

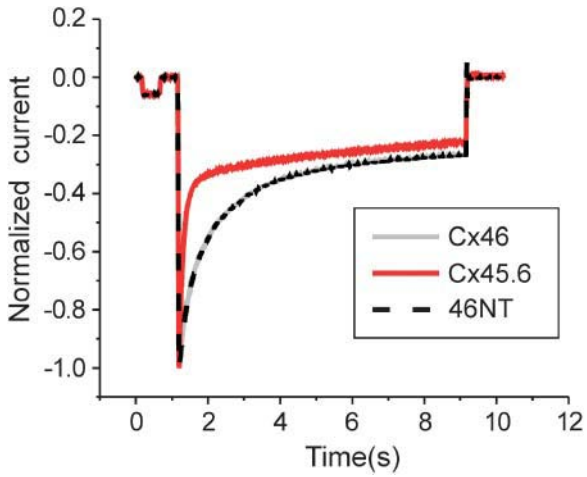

FIGURE 2 Comparison of the time course of inactivation of wild-type and chimeric gap junctional currents. Junctional currents were elicited by transjunctional voltage-clamp steps to −90 mV and normalized with respect to the peak inward current. Note that the time course of Cx46 (*solid gray line*) and 46NT (*dashed line*) are nearly perfectly superimposable.

Molecular dissection of the N-terminus

An alignment of the N-terminus segment across chicken Cx45.6 and species orthologs of Cx46 reveals the presence of seven amino acid residues that are unique to the Cx45.6 sequence (Fig. 4). We therefore mutated these residues, either individually or in combination, to the aligned residues in the Cx46 sequence and expressed the resulting connexins as homotypic gap junctional channels in *Xenopus* oocyte pairs. All of these mutations induced high levels of gap junctional coupling when expressed in oocyte pairs. The mutations R23K, Q17H, and Q13N + V14A + N15Q had little effect on the gating properties of the gap junctional channels whereas the mutation N9R + I10L showed Cx46-like kinetics (data not shown). Additional point mutations identified R9 of Cx46 as the key determinant in the N-terminus. Introducing just this one residue into Cx45.6 produced Cx46-like kinetics (see Table 1) and reduced the voltage sensitivity of the junctional conductance (Fig. 5). The Boltzmann parameters obtained for the point mutant were similar to those determined for the Cx45.6-46NT chimera (Table 2).

Expression of N-terminus mutations in N2A cells

Previous studies of Cx32-Cx26 chimeras suggest that the N-terminus lies within the pore when the channel is open (Verselis et al., 1994; Oh et al., 2000). Thus, changing amino acids in this region might be expected to influence single gap junctional channel conductance as well as channel gating parameters. To test this hypothesis, Cx45.6-46NT and wild-type Cx45.6 were expressed in communication-deficient N2A cells. Dual whole-cell patch-clamp experiments showed that both constructs formed functional gap junctional channels. Fig. 6 compares representative families of macroscopic current traces, *I-V* curves, and normalized steady-state G_j-V_j curves recorded from cell pairs expressing wild-type Cx45.6 or Cx45.6-46NT. The behavior of Cx45.6 and Cx45.6-46NT in N2A cells was similar to that observed in oocytes. One of the main effects of exchanging the N-terminus was to slow the inactivation kinetics. The time course of inactivation of Cx45.6 and 46NT at $V_j = 100$ mV could be described by a single exponential with $\tau = 117.9 \pm 12.1$ ms and 907.5 ± 129 ms, respectively. It also reduced the voltage sensitivity of the steady-state conductance (Table 2).

Fig. 7 *A* shows records from a homotypic Cx45.6 cell pair whose gap junction contained only one function channel. Voltage-clamp pulses of 8 s were applied to cell 1 while cell 2 was held constant at 0 mV. Junctional currents were recorded from cell 2. As illustrated for $V_j = 100$, 90, 70, 60, and 50 mV, the junctional current showed three discrete levels corresponding to the main state (*solid line*), and residual and closed states (*dashed lines*). The amount of time that the channel spent in the main open state was strongly voltage-dependent, becoming extremely small at large

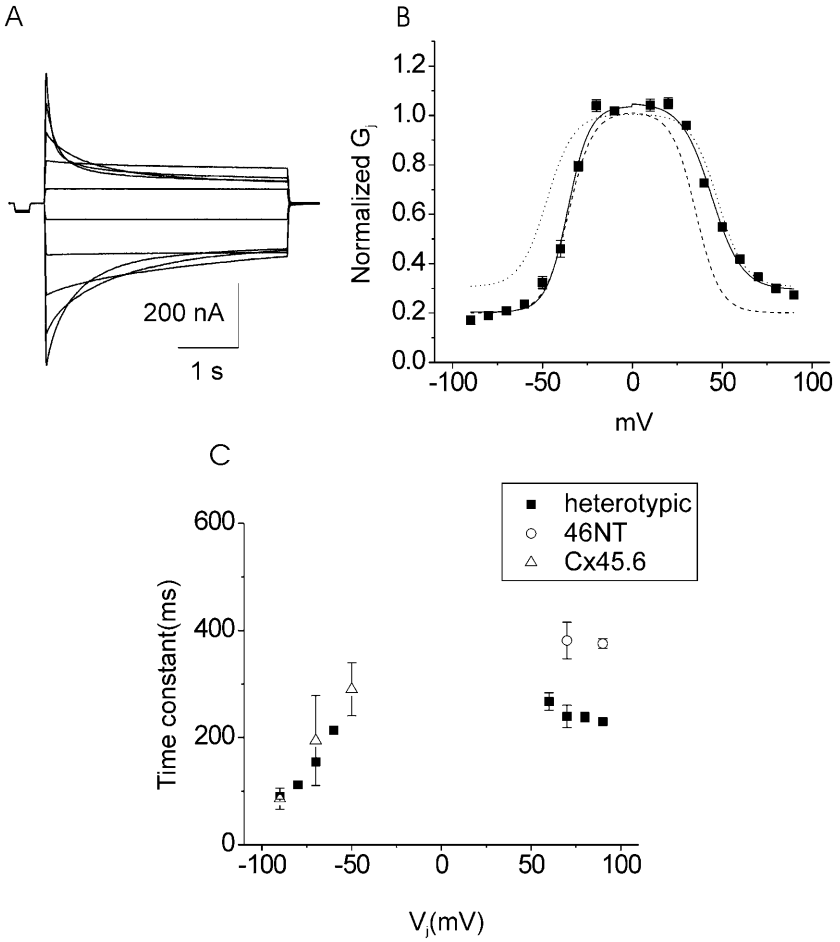

FIGURE 3 Voltage-dependent properties of heterotypic gap junctional channels formed by Cx45.6 and Cx45.6-46NT. (*A*) Recordings of junctional current measured in the Cx45.6 cRNA-injected oocyte in response to 8-s transjunctional voltage-clamp steps between −90 mV and 90 mV applied to the Cx45.6-46NT cRNA-injected oocyte. (*B*) The relationship between the normalized steady-state junctional conductance and V_j (relative to the cell expressing Cx45.6-46NT). Points represent the mean ± SE obtained for five cell pairs. The solid lines are the best fit of the 46NT data to Boltzmann equations whose parameters are given in Table 2. For comparison, the fits to the homotypic data for Cx45.6 (*dashed line*) and 46NT (*dotted line*) are shown. (*C*) Plot of the fast time constant of inactivation (τ_{fast}) versus transjunctional voltage (V_j). τ_{fast} was calculated from biexponential fits to the data for heterotypic 45.6/46NT (*solid squares*), homotypic Cx45.6-46NT (*open circles*), and homotypic Cx45.6 (*open triangles*) pairs.

values of V_j. Fig. 7 *C* shows the unitary *I-V* relationship of the main state for the experiment illustrated in Fig. 7 *A*. The *I-V* relationship of the main state was linear between 90 mS and −90 mV and had a slope conductance, γ_j, of 184 ps. Because of limitations in time resolution, it was not possible to accurately measure the amplitude of the main state for $V_j \geq |100$ mV|. In four cell pairs containing one or two functional channels, $\gamma_{j,main} = 202.4 \pm 9.7$ pS.

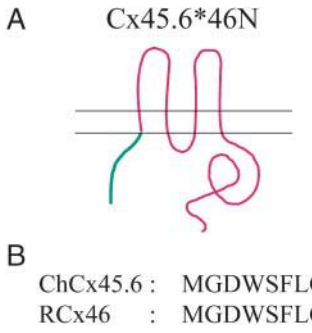

FIGURE 4 (*A*) Schematic representation and membrane topology of chimeric gap junctional proteins made by swapping domains between Cx45.6 (*red*) and Cx46 (*green*). (*B*) Alignment of ChCx45.6 and RCx46 amino acid sequences of the N-terminus.

Exchanging the N-terminus reduced $\gamma_{j,main}$ and altered channel gating kinetics. Fig. 8 *A* shows representative junctional current traces recorded from a Cx45.6-46NT cell pair at $V_j = 100$, 90, 70, 60, and 50 mV. The junctional current exhibited three or four discrete levels corresponding

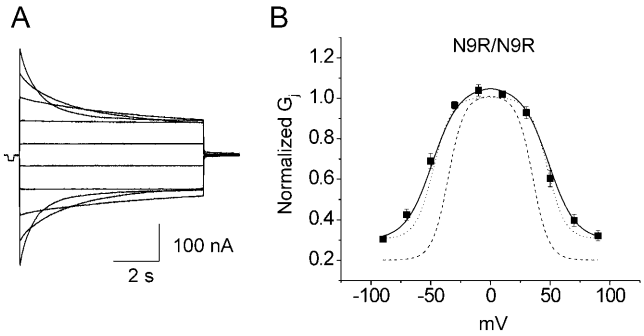

FIGURE 5 Voltage-dependent properties of homotypic gap junctional channels formed by Cx45.6-N9R. (*A*) Junctional current traces recorded in response to 8 s transjunctional voltage-clamp steps between 90 mV and −90 mV. (*B*) The relationship between the normalized steady-state junctional conductance and V_j. Points represent mean ± SE for six cell pairs. The solid lines are the best fit of the heterotypic data to Boltzmann equations whose parameters are given in Table 2. For comparison, the fits to the homotypic data for Cx45.6 (*dashed line*) and 46NT (*dotted line*) are shown.

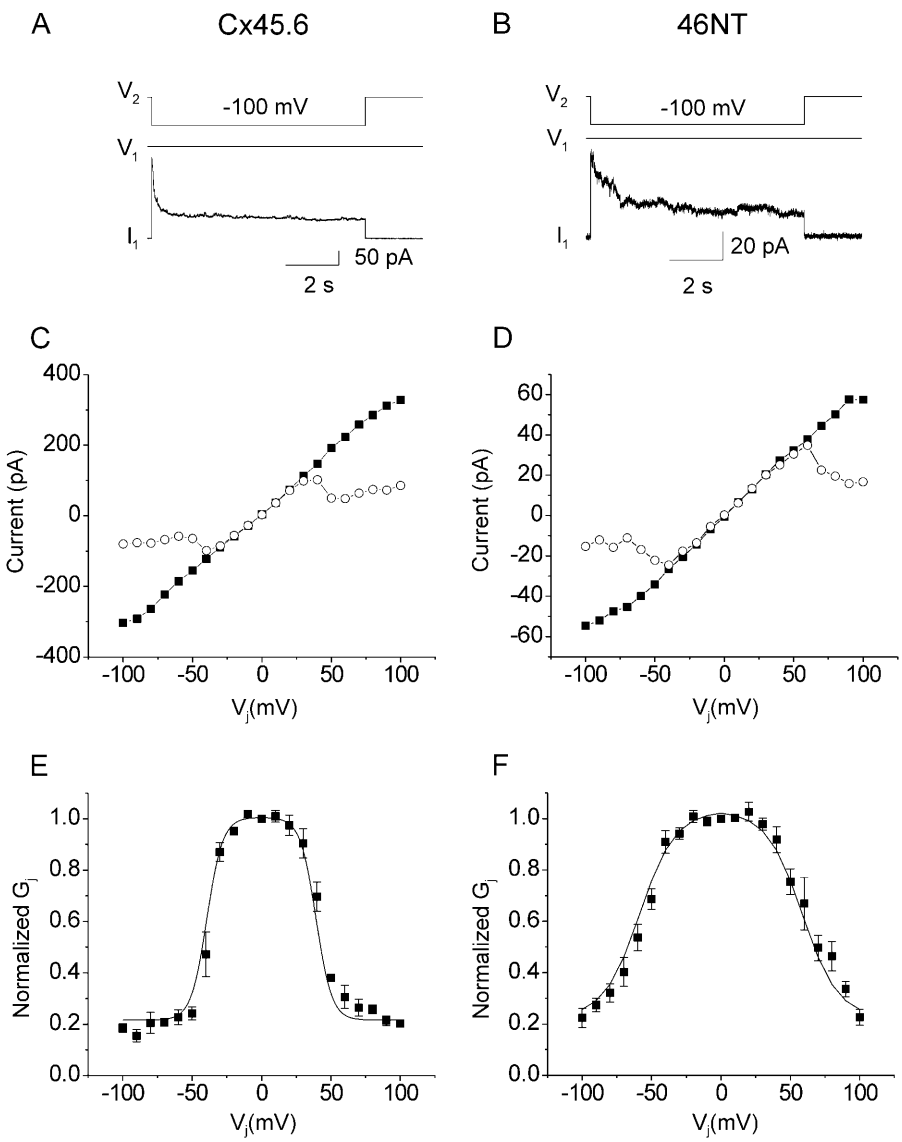

FIGURE 6 Comparison of macroscopic voltage-dependent gating properties of gap junctional channels in N2A cell pairs expressing Cx45.6 or Cx45.6-46NT. (*A* and *B*) Typical multichannel gap junctional current traces recorded from an N2A cell pair expressing wild-type Cx45.6 (*A*) or Cx45.6-46NT (*B*). Junctional currents were elicited by a transjunctional voltage-clamp step to −100 mV. (*C* and *D*) Initial (*solid squares*) and steady-state (*open circles*) I_j-V_j relationships for the cell pairs shown in *A* (*C*) or *B* (*D*). (*E* and *F*) Normalized steady-state gap junctional conductance as a function of transjunctional voltage (V_j) for the cell pairs shown in *A* (*E*) or *B* (*F*). Points represent mean ± SE. The solid line is the best fit of the experimental data (*solid squares*) to Boltzmann equations whose parameters are given in Table 2.

to the main state (*solid line*), and substate 1, substate 2, and closed state (*dashed lines*). Fig. 8 *C* shows the *I-V* relationships for the main state and the subconductance states. In this particular experiment, $\gamma_{j,main} = 116.4$ pS, $\gamma_{j,s1} = 35.2$ pS, and $\gamma_{j,s2} = 17.8$ pS. Analysis of data from eight cell pairs containing one or two functional channels yielded a $\gamma_{j,main} = 129.6 \pm 4.0$ pS, which is significantly reduced compared to that observed for the Cx45.6 channels. Another difference was that the open times for the main conductive state were prolonged compared to those of Cx45.6 (Fig. 9). Recordings at $V_j = \pm 100$ mV yielded a mean open time of 1240.6 ms. In contrast, the mean open time of Cx45.6 channels was 64 ms.

DISCUSSION

Previous studies have shown that gap junctional channels formed from chicken Cx45.6 and rat Cx46 exhibit marked differences in voltage-gating properties. However, until now, the determinants underlying these differences were not known. In this study, we determined the structural basis for this change by constructing a series of Cx45.6-Cx46 chimeras and investigating their voltage-dependent gating properties in the *Xenopus* oocyte pair system. Our results show that the N-terminus is the main determinant because replacing the N-terminus of Cx45.6 with the corresponding one for Cx46 slows the inactivation kinetics of the resultant chimeric gap junctional channels so that they resemble those of Cx46 and decreases the V_j-sensitivity of the steady-state junctional conductance. Furthermore, dual whole-cell patch-clamp experiments of N2A cell pairs expressing wild-type Cx45.6 or 46NT reveal that the N-terminus is an important determinant of single-channel conductance. Wild-type Cx45.6 junctional channels have a main-state conductance of 202 pS, which is similar to the values previously reported for mouse and human Cx50 (Srinivas et al., 1999; Xu and Ebihara, 1999). Exchanging the

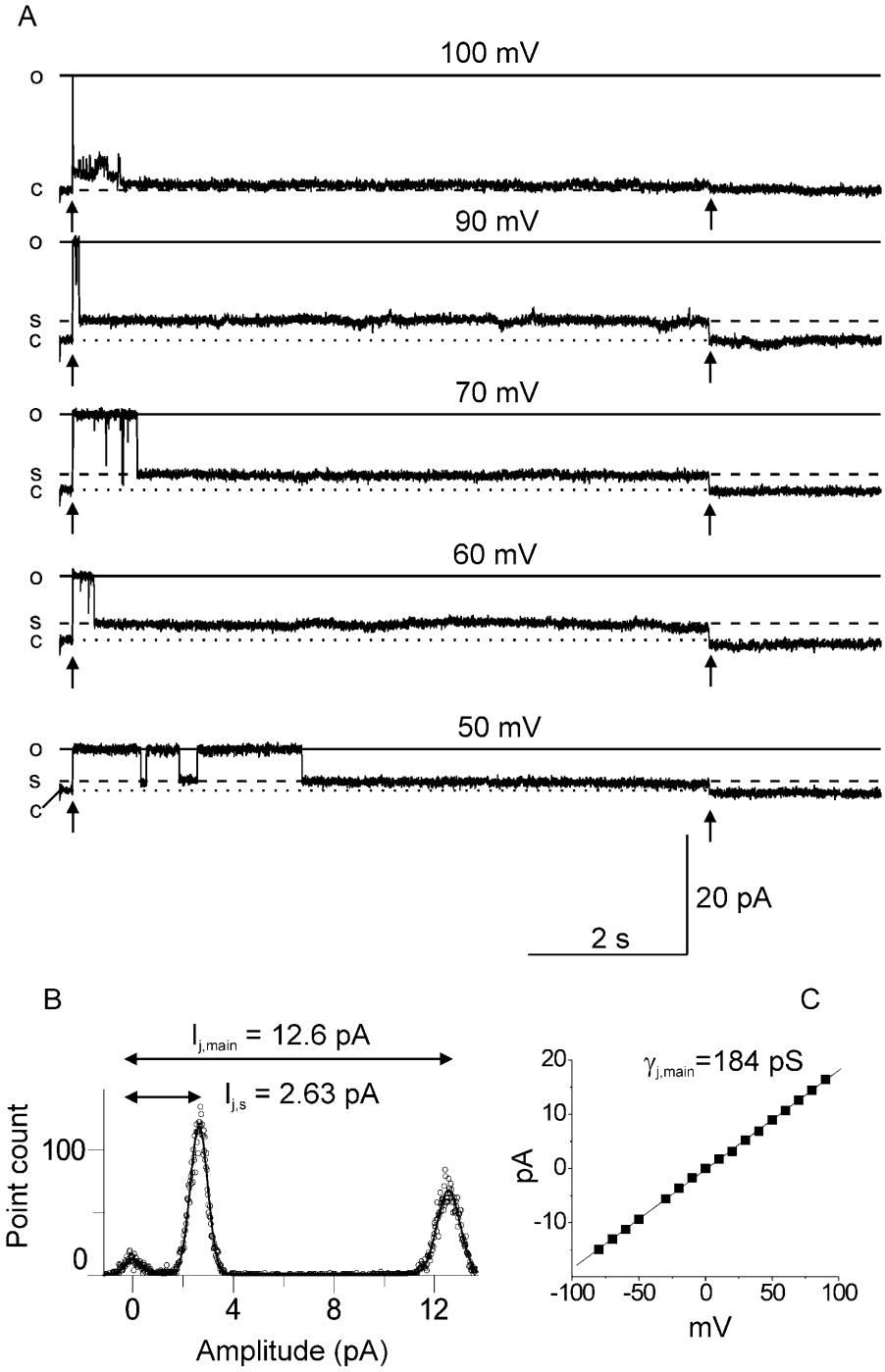

FIGURE 7 Single-channel conductance of wild-type Cx45.6 gap junctional channels. (*A*) Junctional current traces recorded in response to transjunctional voltage-clamp steps to the indicated potentials. Single channels opened to their maximum value (*O*) from the baseline level (*C*) immediately after application of a voltage-clamp step, and then closed to a prolonged subconductance state (*S*). Arrows indicate the beginning and end of the transjunctional voltage clamp steps. (*B*) The all-points histogram and corresponding fit to Gaussian functions for the current recordings obtained at $V_j = 70$ mV. (*C*) *I-V* relationship for the main open state of the gap junctional channel shown in *A*.

N-terminus of Cx45.6 with that of Cx46 reduces the main-state conductance to 130 pS, which is similar to the value previously reported for Cx46 (Hopperstad et al., 2000).

We attempted to identify discrete determinants within the N-terminus by constructing a series of chimeras in which we introduced short segments of Cx46 sequence into the Cx45.6 template. Our results identified a uniquely occurring arginine at position 9 in Cx46 as the main determinant in the N-terminus. Introducing just this one amino acid into the N-terminus of Cx45.6 could account for most of the changes in voltage-gating properties of the gap junctional channels. R9 is conserved in all of the Cx46 species orthologs and is absent in Cx45.6 and other species orthologs of Cx50, supporting its key role in determining the voltage-dependent gating properties and single-channel conductance of the lens fiber connexins.

It should be mentioned that although the N-terminus could account for most of the functional differences observed

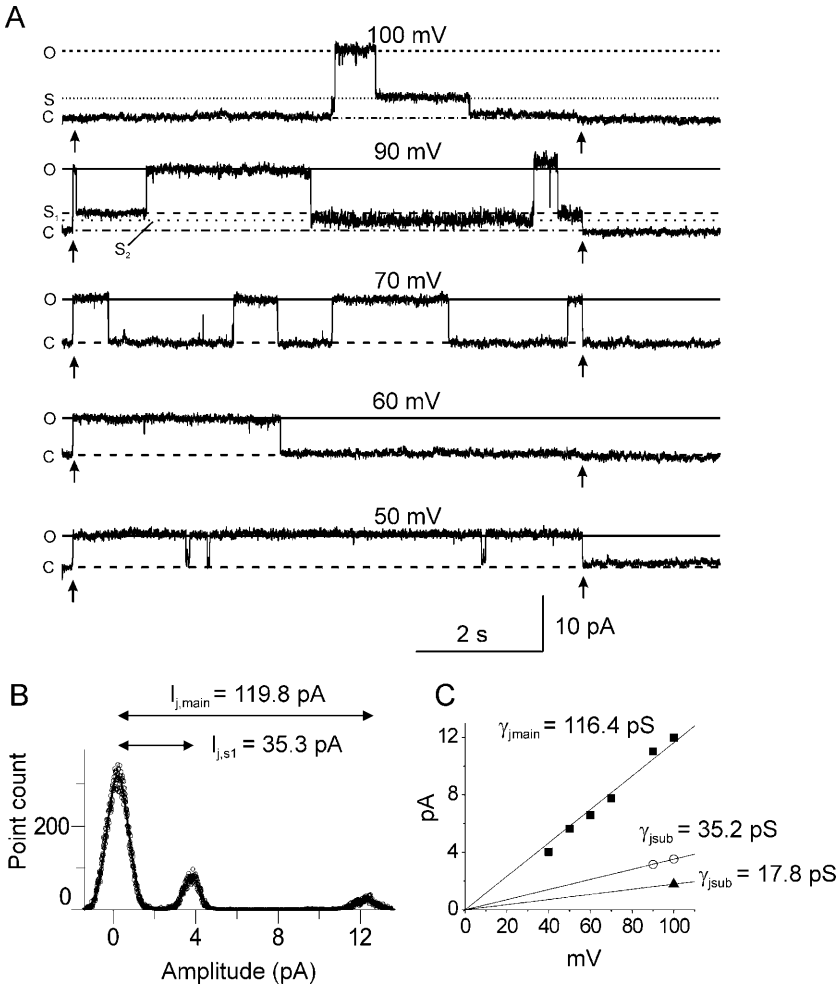

FIGURE 8 Single-channel conductance of Cx45.6-46NT gap junctional channels. (*A*) Junctional current traces recorded in response to transjunctional voltage-clamp steps to the indicated potentials. Arrows indicate the beginning and end of the transjunctional voltage-clamp steps. The main open state and closed state are labeled O and C, respectively, and the substates are labeled S_1 and S_2. (*B*) The all-points amplitude histogram and corresponding fit to Gaussian functions for the current recordings obtained at $V_j = 100$ mV. (*C*) *I-V* relationships for the main open state and the substates of the gap junctional channel shown in *A*.

between Cx45.6 and Cx46, it could not account for all of them. For example, the steady-state junctional conductance of the Cx45.6-46NT had a voltage sensitivity that was intermediate between that of Cx45.6 and Cx46. This suggests that there are other regions of the connexin besides the N-terminus that contribute to voltage gating.

To better understand how the V_j -gating properties of the gap junctional channels are derived from the gating properties of their component hemichannels, we compared the macroscopic voltage-gating properties of heterotypic Cx45.6/46NT gap junctional channels with those of the corresponding homotypic junctional channels. Junctional currents from Cx45.6/46NT cell pairs showed asymmetric voltage-dependent closure, characterized by a faster time course when V_j was positive with respect to the Cx45.6 oocyte. The steady-state G_j-V_j relationship was also asymmetric. The junctional

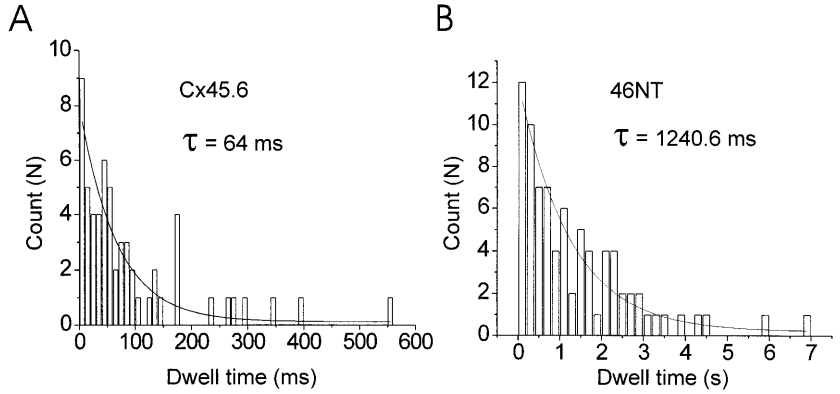

FIGURE 9 Open dwell time histograms for Cx45.6 (*A*) and Cx45.6-46NT (*B*) channels. $V_j = 100$ mV. Closed times <20 ms were ignored during the data analysis.

conductance declined more steeply at positive transjunctional voltages relative to the Cx45.6 oocyte. Similar results were obtained for heterotypic Cx45.6/N9R junctional cell pairs (data not shown). This behavior could be predicted from that of the homotypic channels if it is assumed that in a gap junction, the component hemichannels function independently and that both hemichannels close in response to positive potential.

It has been previously proposed that a portion of the N-terminus lies within the pore of the channel when the channel is open and can sense membrane field, and that movement of the N-terminus toward the cytoplasm causes the channel to close (Verselis et al., 1994; Oh et al., 2000). According to this model, replacing a neutral residue with a positively charged one would make the N-terminus of the Cx45.6 subunit less negative and thus would be predicted to reduce the V_j sensitivity of Cx45.6 in agreement with our experimental data. The addition of a positive charge near the cytoplasmic end of the Cx45.6 hemichannel pore would also depress the entry of cations into the channel and could account for the experimentally observed reduction in the unitary conductance of the main open state in homotypic 46NT/46NT cell pairs. An important question that remains to be addressed is whether exchanging the N-terminus alters the channel's permeability to biological relevant signaling molecules. It would also be interesting to determine if genetic replacement of the coding region of the rodent version of Cx45.6 with a chimera containing the N-terminus of Cx46 modifies ocular growth or leads to the development of cataracts in mice.

This study was supported by National Institutes of Health grant EY10589 (to L.E.).

REFERENCES

Beahm, D. L., and J. E. Hall. 2002. Hemichannel and junctional properties of connexin 50. *Biophys. J.* 82:2016–2031.

Bennett, M. V. L., L. C. Barrio, T. A. Bargiello, D. C. Spray, E. Hertzberg, and J. C. Saez. 1991. Gap junctions: new tools, new answers, new questions. *Neuron.* 6:305–320.

Beyer, E. C., D. L. Paul, and D. A. Goodenough. 1987. Connexin43: a protein from rat heart homologous to a gap junction protein from liver. *J. Cell Biol.* 105:2621–2629.

Ebihara, L. 1992. Expression of gap junction proteins in *Xenopus* oocyte pairs. *In* Ion Channels. B. Rudy and L. E. Iverson, editors. Academic Press, San Diego, CA. 376–380.

Ebihara, L. 1996. *Xenopus* connexin38 forms hemi-gap-junctional channels in the nonjunctional plasma membrane of *Xenopus* oocytes. *Biophys. J.* 71:742–748.

Ebihara, L., and E. Steiner. 1993. Properties of a nonjunctional current expressed from a rat connexin46 cDNA in Xenopus oocytes. *J. Gen. Physiol.* 102:59–74.

Eckert, R. 2002. pH gating of lens fibre connexins. *Pflugers Arch.* 443: 843–851.

Gong, X., E. Li, G. Klier, Q. Huang, Y. Wu, H. Lei, N. M. Kumar, J. Horwitz, and N. B. Gilula. 1997. Disruption of α_3 connexin gene leads to proteolysis and cataractogenesis in mice. *Cell.* 91:833–843.

Hopperstad, M. G., M. Srinivas, and D. C. Spray. 2000. Properties of gap junction channels formed by Cx46 alone and in combination with Cx50. *Biophys. J.* 79:1954–1966.

Jiang, J. X., T. W. White, D. A. Goodenough, and D. L. Paul. 1994. Molecular cloning and functional characterization of chick lens fiber connexin 45.6. *Mol. Biol. Cell.* 5:363–373.

Mackay, D., A. Ionides, Z. Kibar, G. Rouleau, V. Berry, A. Moore, A. Shiels, and S. Bhattacharya. 1999. Connexin46 mutations in autosomal dominant congenital cataract. *Am. J. Hum. Genet.* 64:1357–1364.

Musa, H., E. Fenn, M. Crye, J. Gemel, E. C. Beyer, and R. D. Veenstra. 2004. Amino terminal glutamate residues confer spermine sensitivity and affect voltage gating and channel conductance of rat connexin40 gap junctions. *J. Physiol.* 557:863–878.

Neyton, J., and A. Trautmann. 1985. Single channel currents of an intercellular junction. *Nature.* 317:331–335.

Oh, S., C. K. Abrams, V. K. Verselis, and T. A. Bargiello. 2000. Stoichiometry of transjunctional voltage-gating polarity reversal by a negative charge substitution in the amino terminus of a connexin32 chimera. *J. Gen. Physiol.* 116:13–31.

Paul, D. L., L. Ebihara, L. J. Takemoto, K. I. Swenson, and D. A. Goodenough. 1991. Connexin46, a novel lens gap junction protein, induces voltage-gated currents in nonjunctional plasma membrane of *Xenopus* oocytes. *J. Cell Biol.* 115:1077–1089.

Purnick, P. E., S. Oh, C. K. Abrams, V. K. Verselis, and T. A. Bargiello. 2001. Reversal of the gating polarity of gap junctions by negative charge substitutions in the N-terminus of connexin 32. *Biophys. J.* 79:2403–2415.

Sakai, R., C. Elfgang, R. Vogel, K. Willecke, and R. Weingart. 2003. The electrical behaviour of rat connexin46 gap junction channels expressed in transfected HeLa cells. *Pflugers Arch.* 446:714–727.

Shiels, A., D. Mackay, H. Irisawa, V. Berry, A. Moore, and S. Bhattacharya. 1998. A missense mutation in the human connexin50 gene (GJA8) underlies autosomal dominant ''Zonular Pulverulent'' cataract, on chromosome 1q. *Am. J. Hum. Genet.* 62:526–532.

Spray, D. C., A. L. Harris, and M. V. L. Bennett. 1981. Equilibrium properties of voltage dependent junctional conductance. *J. Gen. Physiol.* 77:77–93.

Srinivas, M., M. Costa, Y. Gao, A. Fort, G. I. Fishman, and D. C. Spray. 1999. Voltage dependence of macroscopic and unitary currents of gap junction channels formed by mouse connexin50 expressed in rat neuroblastoma cells. *J. Physiol.* 517:673–689.

Verselis, V. K., C. S. Ginter, and T. A. Bargiello. 1994. Opposite voltage gating polarities of two closely related connexins. *Nature.* 368:348–351.

White, T. W. 2002. Unique and redundant connexin contributions to lens development. *Science.* 295:319–320.

White, T. W., R. Bruzzone, D. A. Goodenough, and D. L. Paul. 1992. Mouse Cx50, a functional member of the connexin family of gap junction proteins, is the lens fiber protein MP70. *Mol. Biol. Cell.* 3: 711–720.

White, T. W., R. Bruzzone, S. Wolfram, D. L. Paul, and D. A. Goodenough. 1994. Selective interactions among the multiple connexin proteins expressed in the vertebrate lens: the second extracellular domain is a determinant of compatibility between connexins. *J. Cell Biol.* 125:879–892.

White, T. W., D. A. Goodenough, and D. L. Paul. 1998. Targeted ablation of connexin50 results in micropthalmia and zonular pulverulent cataracts. *J. Cell Biol.* 143:815–825.

Willecke, K., J. Eiberger, J. Degen, D. Eckardt, A. Romualdi, M. Guldenagel, U. Deutsch, and G. Sohl. 2002. Structural and functional diversity of connexin genes in the mouse and human genome. *Biol. Chem.* 383:725–737.

Xu, X., and L. Ebihara. 1999. Characterization of a mouse Cx50 mutation associated with the No2 mouse cataract. *Invest. Ophthalmol. Vis. Sci.* 40:1844–1850.